Preparation of Liquid–Crystal Thermosets: *In Situ* Photopolymerization of Oriented Liquid–Crystal Diacrylates

CHAIN-SHU HSU, HWAI-LEN CHEN

Department of Applied Chemistry, National Chiao Tung University, Hsinchu, Taiwan 30050

Received 15 February 1999; accepted 21 June 1999

ABSTRACT: The photoinitiated polymerization of 2-chloro-1,4-phenylene bis[4-[6-(acryloyloxy)hexyloxy]benzoate] (**1M**) was studied. The monomer **1M** exhibited a broad nematic phase between 24.9 and 113.7 °C on a DSC cooling scan. It was oriented in its nematic phase at a substrate coated with polyimide and unidirectionally rubbed with a nylon cloth. During polymerization, the ordering of the liquid–crystal molecules was fixed, yielding a uniaxially crosslinked network. The clear liquid–crystal networks (LCNs) exhibited a birefringence between 0.14 and 0.19, depending on the polymerization temperature. Finally, a nonmesogenic diluent, tetra(ethylene glycol)diacrylate, was mixed with **1M**, subsequently decreasing the birefringence of the obtained LCNs. The LCNs containing nonmesogenic diluent exhibited not only a smaller birefringence but also a weaker birefringence dispersion in the visible region. © 1999 John Wiley & Sons, Inc. J Polym Sci A: Polym Chem 37: 3929–3935, 1999

Keywords: liquid–crystal network; photopolymerization; compensation film

INTRODUCTION

Oriented liquid–crystal networks (LCNs), an interesting class of polymeric materials, are highly promising for diverse applications. Optical anisotropy is an important property of the oriented liquid–crystalline thermosets (LCTs). This kind of optically anisotropic LCN can be used as an optical compensation film for a liquid–crystal display (LCD) to resolve its narrow-viewing-angle problem.[1–4] Recently, Broer and coworkers,[5–14] Hikmet and coworkers,[15–20] and Hoyle et al.[21] demonstrated that macroscopically oriented LCNs can be obtained by *in situ* photopolymerization of difunctional liquid–crystal monomers (LCMs) in contact with unidirectionally rubbed thin-film substrates. During polymerization, the ordering of the mesogen was fixed, yielding a uniaxially crosslinked network. However, most of the difunctional LCMs reported in the literature exhibited a nematic mesophase only at an extremely high temperature (>100 °C). This make it difficult to prepare the oriented polymer films.

In this study, we synthesized a liquid–crystal (LC) diacrylate showing a wide nematic phase near room temperature. The LC diacrylate was oriented macroscopically in homogeneous and homeotropic arrangements. Photoinitiated polymerization fixed the oriented states rapidly and yielded several kinds of LCNs. Their degree of order was determined by infrared dichroism and birefringence measurements. Finally, a nonmesogenic diacrylate, tetra(ethylene glycol)diacrylate, was mixed with the LC diacrylate to manipulate the birefringence of the obtained LCTs.

EXPERIMENTAL

Materials

Acryloyl chloride, 6-chloro-1-hexanol, 4-hydroxybenzoic acid, 2-chlorohydroquinone, tetra(ethylene glycol)diacrylate, and benzophenone were ob-

Correspondence to: C.-S. Hsu

Journal of Polymer Science: Part A: Polymer Chemistry, Vol. 37, 3929–3935 (1999)
 CCC 0887-624X/99/213929-07

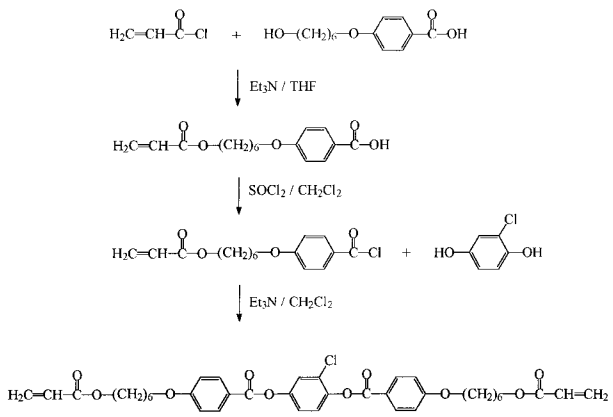

Scheme 1. Synthesis of monomer **1M**.

tained from Aldrich (Milwaukee, WI, USA) and used as received. Dichloromethane used in the esterification reaction was refluxed over calcium hydride and then distilled under nitrogen.

Techniques

^{1}H NMR spectra (300 MHz) were recorded on a Varian (Palo Alto, CA, USA) VXR-300 spectrometer. Thermal transitions and thermodynamic parameters were determined using a Seiko (Chiba, Japan) SSC/5200 differential scanning calorimeter equipped with a liquid-nitrogen cooling accessory. Heating and cooling rates were 10 °C/min. A Carl–Ziess (Oberkochen, Germany) Axiphot optical polarized microscope equipped with a Mettler (Greifensee, Switzerland) FP 82 hot stage and FP 80 central processor was used to observe the thermal transitions and analyze the anisotropic textures. Next, polarized infrared measurements were taken at room temperature on a Perkin–Elmer (Norwalk, CT, USA) 2000 FTIR with a wire-grid polarizer. The wavelength-dependent birefringence of the obtained LCNs was measured by a Otsuka multichannel retardation measuring system RETS-2000 (Osaka, Japan).

Synthesis of the Monomer

The synthesis of the monomer **1M** is outlined in Scheme 1.

4-(6-acryloyloxyhexan-1-oxy)Benzoic Acid (1)

Compound **1** was prepared by esterification of acryloyl chloride with 4-(6-hydroxyhexan-1-oxy)benzoic acid, which was synthesized by etherification of 4-hydroxybenzoic acid with 6-chlorohexanol according to the procedures reported in the literature.[22]

Synthesis of the Monomer 1M

4-(6-Acryloyloxyhexan-1-oxy)benzoic acid (2.0g, 6.85 mmol) was reacted with excess thionyl chloride (2 mL) containing a drop of dimethylformamide in 10 mL of dichloromethane for 2 h. The solvent and excess thiony chloride were removed under reduced pressure to produce the crude acid chloride. Next, the product was dissolved in 8 mL of dichloromethane and added slowly to a cold solution of 2-chlorohydroquinone (0.5 g, 3.46 mmol) and triethylamine (1.30 g, 12.8 mmol) in 50 mL of dichloromethane. The solution was allowed to stir at room temperature for 6 h and then was washed with water and dried over anhydrous $MgSO_4$. After the solvent was removed in a rotary evaporator, the crude product was purified by column chromatography (silica gel, *n*-hexane/dichloromethane = 1/1 as eluent) to yield 2.09 g (88.1%) of white crystals.

^{1}H NMR($CDCl_3$, TMS, ppm, δ): 1.40–1.82 (m, 16H, two —(C$\underline{H}_2$)$_4$—), 4.04 (t, 4H, two —Ph—O—C$\underline{H}_2$—), 4.18 (t, 4H, two —COO—C$\underline{H}_2$—), 5.80 and 6.18 (2d, 4H, two C$\underline{H}_2$═), 6.18 (dd, 2H, two ═C$\underline{H}$—), 7.31 (m, 3H, —O—C$_6\underline{H}_3$(Cl)—O—), and 7.00 and 8.15 (2d 8H, two —O—C$_6\underline{H}_4$—COO—).

Polymerization Procedures

Benzophenone was used as a photoinitiator. Monomer mixtures containing a nonmesogenic diluent were prepared by adding 10 to 40 mol % of tetra(ethylene glycol)diacrylate to the monomer **1M**. The polymerization mixtures were made by dissolving 99 wt % of the monomer **1M** or monomer mixture and 1 wt % of benzophenone in dichloromethane and subsequent evaporation of the solvent under vacuum.

The polymerization mixtures were oriented macroscopically in a glass test cell provided with rubbed polyimide layers. The cell was filled by a capillary flow at 50 °C. The cell thickness was around 6 μm. The monomer was oriented macroscopically in homogeneous and homeotropic arrangements. The oriented monomers were polymerized with a UV intensity of 9 mw/cm^2 at 350 nm, yielding transparent polymer networks with a perfect macroscopic orientation.

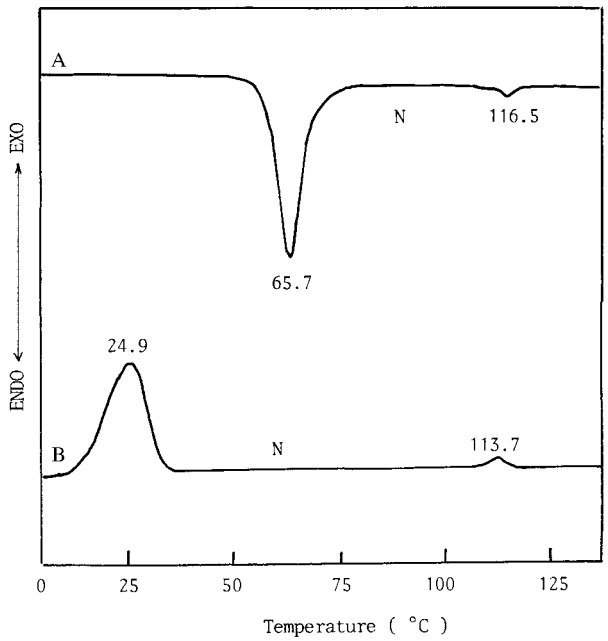

Figure 1. DSC thermograms (10 °C/min) of the monomer **1M**: (A) heating scan and (B) cooling scan.

RESULTS AND DISCUSSION

Mesomorphic Behavior of the Monomer 1M

Scheme 1 depicts the synthetic route used to prepare the monomer **1M**. Figure 1 presents the DSC thermograms of the monomer **1M**. This figure reveals a melting transition at 65.7 °C and a nematic to isotropic phase transition at 116.5 °C on the heating scan (Curve A). On the cooling scan, an isotropic to nematic phase appeared at 113.7 °C as well as a crystallization temperature at 24.9 °C. The monomer **1M** possessed an extremely wide nematic temperature range near room temperature. Such a wide range allowed the monomer to be aligned easily in a glass cell provided with uniaxially rubbed polyimide layers.

Polymerization of the Monomer 1M

Macroscopic orientation of the monomers was induced on a rubbed polyimide. The monomer was aligned in homogeneous and homeotropic arrangements. Both samples were maintained at 50°C during the entire polymerization process. In the homogeneous cell, the molecules were aligned in the parallel direction with respect to the glass surface. Therefore, the optical polarizing microscopic observation revealed a monodomain-like texture. This texture was maintained during polymerization. Only a color change occurred because of the slight change in the optical retardation defined by the product of thickness d and birefringence Δn. Figure 2(A) shows the monodomain-like texture exhibited by the homogeneously oriented polymer network. The polymer chain direction is observed clearly in the photograph. Figure 3 presents the X-ray diffraction pattern of the homogeneously oriented polymer network. Two crescents with d spacing of 4.5 Å were observed on the equator. This X-ray result indicates the formation of the uniaxially oriented

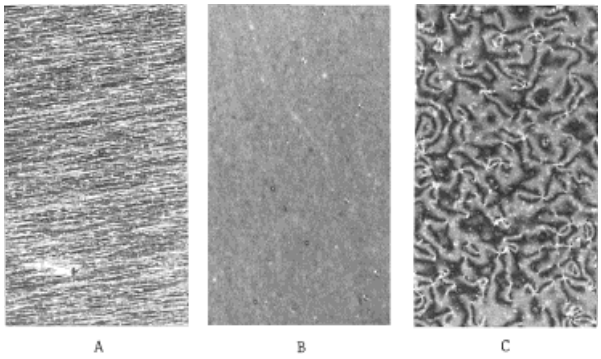

Figure 2. Optical polarizing micrographs displayed by (A) a homogeneously aligned network, (B) a homeotropically aligned network, and (C) an unaligned network.

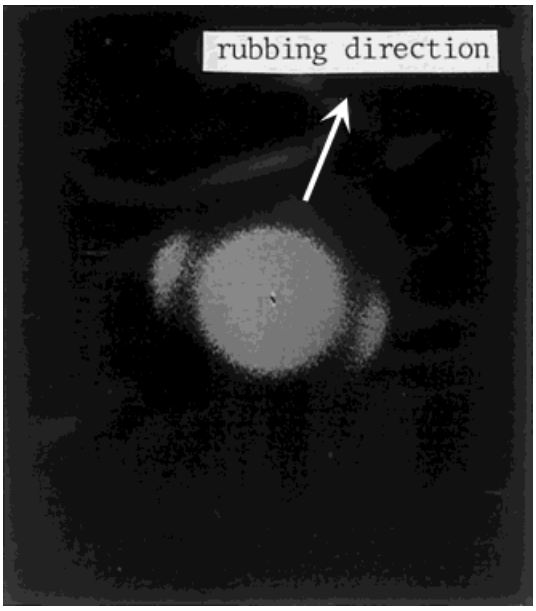

Figure 3. X-ray diffraction pattern of the homogeneously aligned network.

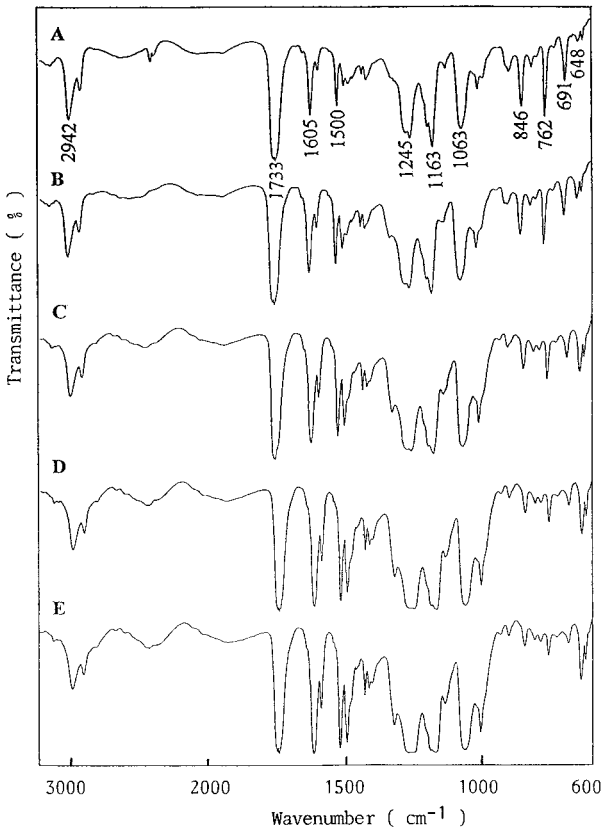

Figure 4. FTIR spectra recorded with the IR light source polarized (A) 90°, (B) 60°, (C) 45°, (D) 30°, and (E) 0° to the rubbing direction for a homogeneously aligned network.

nematic structure in which the molecular axis was parallel to the rubbing direction. In the homeotropic cell, the molecules were aligned in a perpendicular direction with respect to the glass surface, and the optical polarizing microscopic observation showed a complete dark texture [Fig. 2(B)] during polymerization. For the unaligned sample, the molecules were arranged as a polydomain nematic texture at 50 °C. This nematic texture was maintained during polymerization. Figure 2(C) shows the typical nematic schlieren texture exhibited by the unaligned polymer network. The monomer **1M** crystallized at a temperature below 24.5 °C, and no photopolymerization occurred in the crystalline state.

Figures 4 and 5 present the polarized Fourier transform infrared (FTIR) spectra of homogeneously aligned and homeotropically aligned polymer networks, respectively. For the homogeneously aligned polymer network, the mesogenic units are aligned in the parallel direction with respect to the glass surface. There was a marked

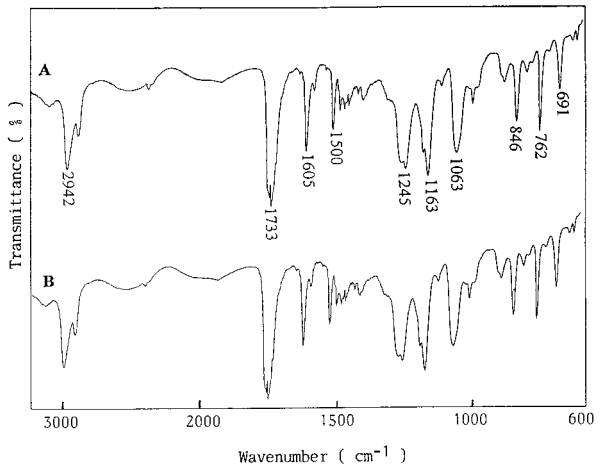

Figure 5. FTIR spectra recorded with the IR light source polarized (A) 90° and (B) 0° to the rubbing direction for a homeotropically aligned network.

difference between the polarized infrared spectrum in the direction of the film orientation and the spectrum recorded with the infrared light source polarized 90° to the rubbing direction [see spectra 4(A) and 34(E)]. Figure 6 plots the band-absorbance ratio versus the infrared polarization angle for several characteristic bands. As the figures reveal, the absorbances at 1,605 cm^{-1} (assigned to a C═C stretching band of the phenyl ring), 1,245 cm^{-1} (assigned to a C—O—C ester stretching band), and 648 (assigned to a C—Cl stretching) gradually decreased as the polarization angle increased from 0 to 90°. However, the absorbances at 2,942 cm^{-1} (assigned to a C—H

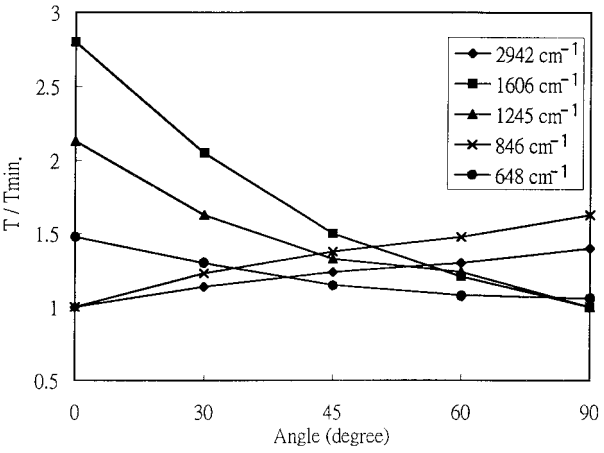

Figure 6. Plot of the ratio of IR absorbance/minimum IR absorbance versus polarization angle for several characteristic IR bands of groups in a homogeneously aligned network.

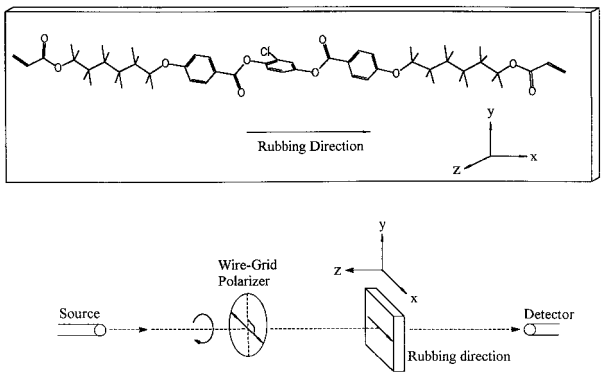

Figure 7. Schematic illustration for the alignment of the monomer **1M** on a polyimide-rubbed glass substrate.

stretching of the methylene groups) and 846 cm^{-1} (assigned to an out of plane bending of phenyl hydrogen atoms) increased to varying extents as a function of the polarization angle. The absorbance of the band at 1,733 cm^{-1} (assigned to carbonyl stretching) was independent of the polarization angle. These results, as illustrated in Figure 7, clearly indicate a marked degree of alignment in the mesogenic groups as well as flexible spacer units in the rubbing direction in the homogeneously aligned LCNs. The orientations of the aromatic C═C, C—O—C, and C—Cl vibrations are predominantly parallel to the rubbing direction, whereas the orientations of the methylene C—H and aromatic C—H vibrations are predominantly perpendicular to the rubbing direction. For the homeotropically aligned polymer network, the mesogenic units are aligned perpendicularly to the glass substrate. The polarized infrared absorption spectra are independent of the angle of the polarized light [see spectra 4(A) and 4(B)]. This result suggests that the orientations of C—H groups in the methylene units and phenyl rings are random in the lateral direction of the mesogenic group.

Optical Anisotropic Properties of the LCNs

LCDs occupy a prominent position in the display field owing to such characteristic features as low voltage, light weight, and low cost. When viewed directly, an LCD provides a high-quality output. At large viewing angles, however, the image degrades and exhibits poor contrast. This phenomenon occurs because LC cells operate by virtue of the birefringent effect exhibited by LC molecules. Various approaches have been proposed so far to improve the viewing-angle characteristics of LCDs.[23–27] Some desirable properties of an optical compensation film for LCDs are (1) sufficient phase retardation, normally $d\Delta n$ (where d denotes the film thickness andΔn the film birefringence) ranging from $\lambda/8$ to $\lambda/2$, depending on the application; (2) ideal phase match with the employed LC so that a good compensation can be achieved over the entire visible range; (3) high optical transparency; and (4) good uniformity. Among those requirements, the phase match between the film and LC over the entire visible spectral region is particularly important. A phase-matched film would compensate the residual phase retardation of the LC cell at an oblique angle for all the wavelengths employed for a full-color display. Consequently, a high contrast would be obtained. Restated, both birefringence Δn and birefringence dispersion are important parameters for a compensation film used in LCDs.

Photoinitiated polymerization of the monomer **1M** in its homogeneously oriented nematic state at five different temperatures led to five anisotropic polymer networks. The obtained LCNs were transparent to visible light without noticeable light scattering in films with a thickness of 6 μm. Figure 8 displays the wavelength-dependent birefringence Δn of the polymer network obtained by photopolymerization of **1M** at 95, 80, 65, 50, and 35 °C. The polymer networks not only possessed an extremely strong Δn dispersion with wavelength but also exhibited a relatively high birefringence Δn between 0.14 and 0.19, depending on the polymerization temperature. Birefringence of a LC compound or an uniaxial polymer network is attributed primarily to the electronic resonance wavelength(λ^*), molecular packing density (N), number of active electrons, order parameter (S), and differential oscillator strength ($f\|^* - f\perp^*$):[28,29]

$$\Delta n = G[\lambda^2\lambda^{*2}/\lambda^2 - \lambda^{*2}] \quad (1)$$

where $G = gNZS\ (f\|^* - f\perp^*)$ and g represents a proportionality constant. From eq 1, the wavelength-dependent birefringence of a uniaxial polymer network is determined mainly by its resonance wavelength λ^*. A longer λ^* not only leads to a higher birefringence but also exhibits a stronger Δn dispersion in the visible region. The monomer **1M** contains three phenyl rings in its mesogen. Its resonance wavelength λ^* should be ex-

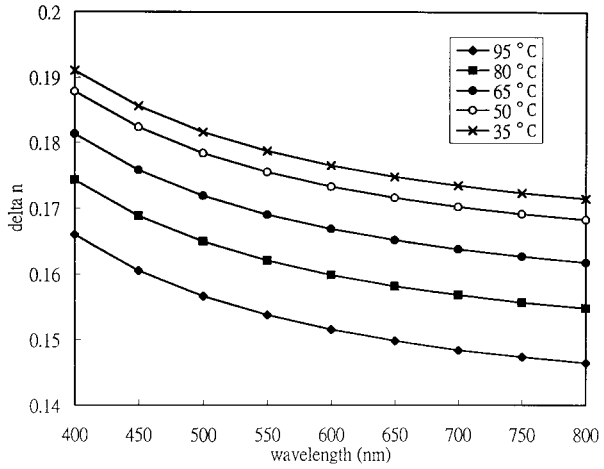

Figure 8. The wavelength-dependent birefringence Δn of the homogeneously alignment networks obtained by photopolymerization of **1M** at 95, 80, 65, 50, and 30°C.

tremely long. This is the reason why the obtained polymer networks exhibited a large birefringence Δn and extremely strong Δn dispersion in the visible region. As can be seen from Figure 8, the birefringence of the LCNs decreased with increasing polymerization temperature. This decrease was expected because when polymerized at a higher temperature, monomer molecules are packed in a lower degree of ordering; consequently, the obtained LCN had a smaller birefringence. This phenomenon implies that the birefringence of the LCNs can be manipulated by controlling the polymerization temperature.

To decrease the birefringence and birefringence dispersion of the LCNs, a nonmesogenic diacrylate, tetra(ethylene glycol)diacrylate, was used to formulate LC mixtures with the monomer **1M**. Figure 8 presents the phase diagrams of the mixtures of tetra(ethylene glycol)diacrylate and **1M**. Figure 9(A,B) shows the phase-transition temperatures obtained respectively from DSC heating and cooling scans. As presented in Figure 9(A), the nematic phase disappeared when 30 mol % of tetra(ethylene glycol)diacrylate was added to the mixture. However, the mixture revealed a nematic phase on the DSC cooling scan even when it contained 40 mol % of tetra(ethylene glycol)diacrylate [Fig. 9(B)]. The LC mixtures were oriented homogeneously in a LC cell and photopolymerized at 50 °C. Figure 10 illustrates the wavelength-dependent birefringence of the LCNs obtained by polymerizing the mixtures of **1M** and tetra(ethylene glycol)diacrylate. Apparently, the birefringence of the LCNs gradually decreased with an increasing nonmesogenic diluent content. The one containing the highest nonmesogenic diluent content exhibited the smallest birefringence. In addition, its birefringence was also more weakly wavelength dependent.

CONCLUSIONS

An LC diacrylate with a wide temperature range of nematic phase near room temperature was synthesized. The LCM was aligned macroscopically in homogeneous and homeotropic arrangements in contact with a unidirectionally rubbed polyimide. Photoinitiated polymerization of the oriented monomer and its mixtures

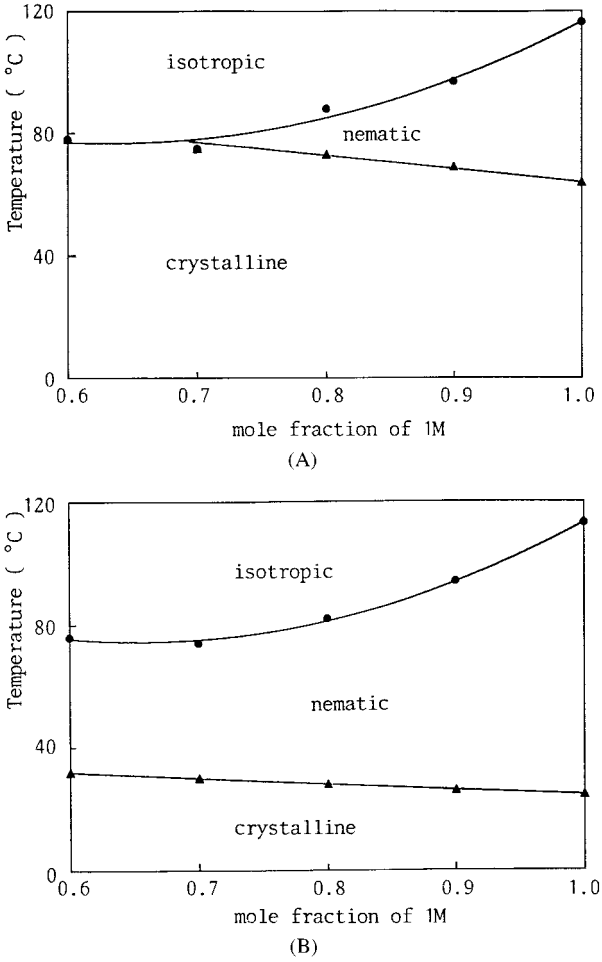

Figure 9. The phase diagrams of the mixtures of **1M** and tetra(ethylene glycol)diacrylate: (A) data obtained from DSC heating scans and (B) data obtained from DSC cooling scans.

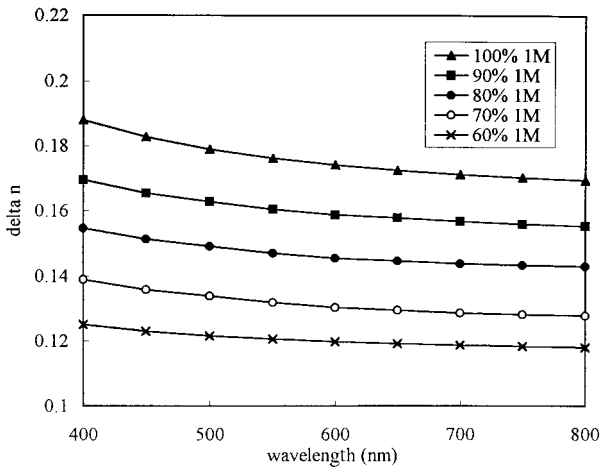

Figure 10. The wavelength dependent birefringence Δn of the homogeneously aligned networks obtained by photopolymerization of the mixtures of **1M** and tetra(ethylene glycol)diacrylate at 50 °C.

with tetra(ethylene glycol) diacrylate yielded transparent polymer networks. In addition, the anisotropic properties of the aligned LC molecules were transferred to their crosslinked networks. Moreover, the obtained LCNs exhibited a large birefringence and a strong birefringence dispersion in the visible region. The birefringence and birefringence dispersion could be manipulated by controlling polymerization temperature and the nonmesogenic diluent content in a LC mixture. The obtained LCNs are highly promising for the optical compensation films in LCDs.

The authors are grateful to the National Science Council of the Republic of China for financial support of this work (NSC Grants 84-2622-E009-012 and NSC 85-2622-E009-011).

REFERENCES AND NOTES

1. Hasebe, H.; Takatsu, H.; Imura, Y.; Kobayashi, S. Jpn J Appl Phys Part 1 1994, 33, 6245.
2. Hasebe, H.; Takeuchi, K.; Takatsu, H. J Soc Inform Display 1995, 3, 139.
3. Ito, Y.; Nishiura, Y.; Kamada, K.; Mori, H.; Nakamura, T. U.S. Patent 5,583,679, 1996.
4. Kawata, K.; Okazaki, M. U.S. Patent 5,518,783, 1996.
5. Broer, D. J.; Finkelmann, H.; Kondo, K. Makromol Chem 1988, 189, 185.
6. Broer, D.; Mol, G. N.; Challa, G. Makromol Chem 1989, 190, 19.
7. Broer, D. J.; Boven, J.; Mol, G. N.; Challa, G. Makromol Chem 1989, 190, 2255.
8. Broer, D. J.; Hikmet, R. A. M.; Challa, G. Makromol Chem 1989, 190, 3201.
9. Broer, D. J.; Mol, G. N.; Challa, G. Makromol Chem 1991, 192, 59.
10. Broer, D. J.; Heyndericky, I. Macromolecules 1990, 23, 2474.
11. Hikmet, R. A. M.; Broer, D. J. Polymer 1991, 32, 167.
12. Heyndericky, I.; Broer, D. J. Mol Cryst Liq Cryst Technol Sect A 1991, 203, 113.
13. Hikmet, R. A. M.; Lub, J.; Broer, D. J. Adv Mater 1991, 3, 392.
14. Broer, D. J.; Lub, J.; Mol, G. N. Macromolecules 1993, 26, 1244.
15. Hikmet, R. A. M.; Zwerrer, B. H. Mol Cryst Liq Cryst Technol Sect A 1991, 200, 197.
16. Hikmet, R. A. M. Liq Cryst 1991, 9, 405.
17. Hikmet, R. A. M.; Lub, J.; Maassen vd Brink, P. Macromolecules 1992, 25, 4194.
18. Hikmet, R. A. M. Macromolecules 1992, 25, 5759.
19. Hikmet, R. A. M.; Zwerver, B. H.; Lub, J. Macromolecules 1994, 27, 6722.
20. Hikmet, R. A. M.; Lub, J.; Tol, A. J. W. Macromolecules 1994, 28, 3313.
21. Hoyle, C. E.; Watanabe, T.; Whitehead, J. B. Macromolecules 1995, 27, 6581.
22. Portugall, M.; Ringsdorf, H.; Zentel, R. Makromol Chem 1982, 183, 2311.
23. Tako, Y.; Sugiyama, T.; Katah, K.; Iimura, Y.; Kobayashi, S. J Appl Phys 1993, 74, 2071.
24. Wu, S. T.; Lackner, A. M. Appl Phys Lett 1994, 64, 2047.
25. Wu, S. T. J Appl Phys 1994, 76, 5975.
26. Harris, F. W.; Cheng, S. Z. D. U.S. Patent 5,480,964, 1996.
27. Wu, S. T. Mater Chem Phys 1995, 42, 163.
28. Wu, S. T. Phys Rev 1986, 33, 1270.
29. Wu, S T. Appl Phys Lett 1981, 69, 2680.